

FABRICATION AND CHARACTERIZATION OF 4-AMINO-6-HYDROXY-2-MERCAPTOPYRIMIDINE STABILIZED GOLD NANOPARTICLES FOR ELECTROCATALYTIC APPLICATION OF EPINEPHRINE AND URIC ACID

F. AJESH^a, S. B. REVIN^{b*}, R. RAVI^c

^aResearch Scholar, Department of Computer Science and Engineering, Francis Xavier Engineering College, Vannarpettai, Tirunelveli 627003, Tamilnadu, India,

^bAnna University Recognized Research Centre, Faculty of Science, Department of Chemistry, Francis Xavier Engineering College, Vannarpettai, Tirunelveli 627003, Tamilnadu, India

^cAnna University Recognized Research Centre, Faculty of Engineering, Department of Computer Science and Engineering, Francis Xavier Engineering College, Vannarpettai, Tirunelveli 627003, Tamilnadu, India

The synthesized 4-amino-6-hydroxy-2-mercapto pyrimidine stabilized gold nanoparticles (AHMP-AuNPs) are tested in different pH conditions (pH3- pH9) to find best optimization point of stabilization. The presence of lone pairs of electrons in the amine groups of the monomer (AHMP) generate the electrostatic repulsion between the adjacent AuNPs surfaces which stabilized from aggregation of AHMP-AuNPs. At neutral pH (pH 7), there is no influence of H⁺ and OH⁻ ions and hence AHMP-AuNPs are well stabilized by their capping agent. Further, the morphology of AHMP-AuNPs is investigated by High resolution transmission electron microscopy (HR-TEM) and X-ray diffraction (XRD). The Bragg reflections of 2θ are 38.1, 44.2, 64.6 and 77.4 indicating the AHMP-AuNPs exist in the lattice space of 111, 200, 220 and 311. Further, AHMP-AuNPs are fabricated on Indium Tin oxide (ITO) electrode using (3-mercaptopropyl)trimethoxysilane (MPTS) linker and the surface was probed by AFM images and it shows 400 nm thickness of layer. The prepared AHMP-AuNPs/MPTS/ITO electrode is used for the electrocatalytic application of epinephrine (EP) and uric acid (UA). Cyclic voltammograms shows the oxidation redox peak for EP with a potential difference of 80 mV and give the oxidation peak for UA at 0.51 V. The simultaneous determination of EP and UA is also was successfully achieved by using the modified electrode. The oxidation peak obtained for EP at 0.15 V and UA at 0.34 V at modified electrode by DPV method.

(Received August 23, 2019; Accepted September 28, 2019)

Keywords: 4-amino-6-hydroxy-2-mercapto pyrimidine stabilized gold nanoparticles, XPS, TEM, AFM, Epinephrine, Uric acid

1. Introduction

Recently, nanoparticles are one of the fashionable and versatile material to modify the substrates due to its electron receiving capacity. It is well-known that the AuNPs can be act as an 'electron antenna' which form conducting channels that facilitate the electron transfer. Hence, the conductivity of the overall modified system will be increase. Especially gold nanoparticles (AuNPs) have promised efficiency enhancement in all the application point of view compared to other nanoparticles [1]. AuNPs are used for biomedical application [2], drug delivery application [3], theranostic agent [4], catalytic application [5], colorimetric detection [6], 3-d printing application [7]. Recently, 4-amino-6-hydroxy-2-mercapto pyrimidine stabilized gold nanoparticles (AHMP-AuNPs) was utilized for the electrochemical detection of tannic acid [8] and vitamin B1 detection by spectrofluorimetry [9]. Epinephrine (EP) is excitomotor of α and β receptor and it is used for the treatment of Coronary Artery disease, hypertension and Asthma [10-12]. Hence, the

*Corresponding author: revin84@gmail.com

determination of EP is very essential from the diseases. The concentration of uric acid (UA) is related to many diseases such as gout [13-14], etc., Moreover, UA is the major interference to EP while determine it because EP and UA exist in human fluids. Hence, simultaneous determination of EP and UA are essential for finding diseases.

Indium tin oxide (ITO) substrate can be operational as a working electrode in a wide potential window and also possess stable electrochemical behaviour. It is best choice of electrode, when we need high potential window for sensor applications. In this present study, we have planned to check the pH effect of AHMP-AuNPs to better understand of its stability. Further, the study is extended to salt effect and also morphological investigations by HR-TEM and XRD. Finally the AHMP-AuNPs modified MPTS-ITO electrode is probed by AFM and its used for the electrocatalytic determination of EP and UA.

2. Experimental

2.1. Materials and chemical equipments

All the chemicals were used in A.R grade. 4-amino-6-hydroxy-2-mercapto pyrimidine, Hydrogen tetrachloroaurate trihydrate ($\text{HAuCl}_4 \cdot 3\text{H}_2\text{O}$), (3-mercaptopropyl) trimethoxysilane (MPTS) were purchased from Sigma-Aldrich and Sodium borohydride (NaBH_4) and sodium chloride (NaCl) were purchased from Merck (India). Different phosphate buffer pH solutions (pH 3-pH9) were prepared using Na_2HPO_4 and NaH_2PO_4 (0.2 mol/L). UV-visible absorption is obtained from JASCO V 630 UV-visible Spectrophotometer. HR-TEM images obtained from a JEOL JEM 3010 model. X-ray diffraction (XRD) was recorded with a D2 phaser Bruker model. AFM images were recorded by Digital Instruments Nanoscope IV, Veeco. Electrochemical measurements were done by CHI electrochemical workstation model 643B (Austin, TX, USA). ITO electrode was used as a working electrode; platinum wire was used as counter electrode and Ag/AgCl (saturated NaCl) electrode used as a reference electrode. Cyclic voltammograms (CV) experiments were carried out at the scan rate of 50 mV s^{-1} . For DPV measurements, pulse width of 0.06 s, amplitude of 0.05 V, sample period of 0.02 s and pulse period of 0.20 s were used. The electrochemical measurements were performed under nitrogen atmosphere at room temperature.

2.2. Preparation of AHMP-AuNPs & its modification

AHMP-AuNPs was prepared by our synthesis method [8]. 0.5 mL of 31.7 mmol/L HAuCl_4 and 0.25 mL of 1 mmol/L 4-amino-6-hydroxy-2-mercapto pyrimidine (AHMP) were added into 23.5 mL of water. After that, the addition of 2 mL of ice cold NaBH_4 (0.125%) in to the same solution with a condition of constant stirring was maintained. When the color changes to wine red from yellow, is indicating that the formation of AHMP-AuNPs. Further, this solution is stir for 20 minutes and stored at 4°C . Further, AHMP-AuNPs solution is adjusted to pH3-pH9 by adding of phosphate buffer. The optimized pH value (pH 7) of AHMP-AuNPs was utilized for dry coating on MPTS for the sensor applications.

(3-mercaptopropyl)trimethoxysilane (MPTS) sol-gel was prepared by our reported method using methanol and water (as 0.1 mol/L HCl) in a molar ratio of 1:3:3 and stirring the mixture for 30 min. Then the cleaned ITO electrode (geometric area 0.012 m²) was immersed for 20 min. After that, the MPTS modified electrode was immersed in AHMP-AuNP solution for 12 hours. The resultant electrode can be abbreviated as AHMP-AuNPs/MPTS/ITO electrode and utilized for the electrocatalytic application.

3. Results and discussions

3.1. pH Studies of AHMP-AuNPs by UV-visible spectroscopy

In our earlier studies, we have proved the synthesis methodology of AHMP-AuNPs by UV-Visible spectroscopy [8]. In this work, we have optimized the exact pH value for the synthesis of AHMP-AuNPs to the benefit of electrocatalytic application. The ideal formation of the AHMP-AuNPs can be tested in different pH. Fig. 1 shows that the UV-visible spectra obtained

for AHMP-AuNPs with different pH values. In neutral pH (pH 7), the AHMP-AuNPs shows a sharp SPR band at 518 nm with high intensity. Since the lone pairs of electrons are present in the amine groups of the monomer (AHMP), creating electrostatic repulsion between the adjacent AuNPs surfaces. Hence, the overall AHMP-AuNPs are stabilized from aggregation. At neutral pH, there is no H^+ and OH^- ions present in the solution and hence no influence applied by those ions. The electrostatic repulsion force is observed at neutral pH, the AHMP-AuNPs are completely stabilized at pH 7. Hence, UV-Visible spectrum is moved towards lesser wavelength at maximum.

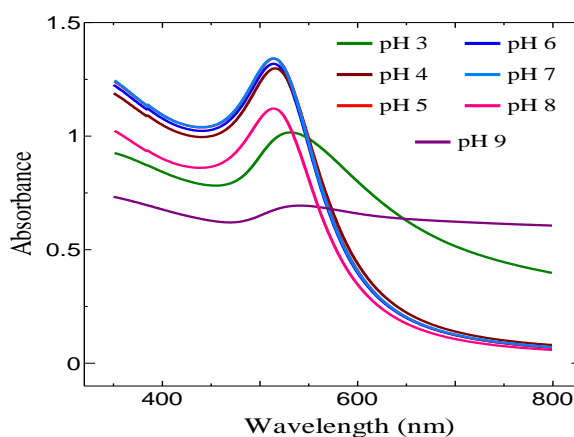


Fig. 1. UV-Visible spectra obtained for AHMP-AuNPs at different pH values of 3, 4, 5, 6, 7, 8 and 9.

In low acidic pH (pH 3), the AHMP-AuNPs shows a broad SPR band around 540 nm with low intensity which indicates the red shift (22 nm) due to the aggregation formation of AHMP-AuNPs particles. In low acidic pH, more H^+ ions are present in the solution which are attracted towards the lone pair of electrons of amine groups of the monomer compound. Hence, the electrostatic repulsion between the adjacent AHMP-AuNPs is reduced which leads to the formation of aggregation. In pH 4, the AHMP-AuNPs provides a sharp SPR band at 522 nm with high intensity. The observed blue shift (18 nm) indicates that the AHMP-AuNPs are not in aggregation form rather than pH 3. This is because the H^+ ion counts are decreased while increasing pH which is possible to increase the electrostatic repulsion between AHMP-AuNPs.

Hence, UV-Visible peak shifts towards the lesser wavelength side. In pH 5, the AHMP-AuNPs shows a sharp peak at 521 nm with high intensity which indicates that the ideal condition of the AHMP-AuNPs stabilization goes better and better. In pH 6, AHMP-AuNPs gives the sharp peak at 520 nm with high intensity. On the other hand, high basic pH (pH 9), the AHMP-AuNPs shows a hump around 550 nm which implies that the strong aggregation of AHMP-AuNPs. The reason behind is high basic solution has more OH^- ions which induce the negative-negative repulsion with the lone pair of electrons of the monomer's amine group in AHMP-AuNPs. Hence, the electrostatic repulsion between adjacent lone pairs of electrons in AHMP-AuNPs is forced to reduce due to the formation of new negative-negative repulsion by OH^- . It makes the possibility of the adjacent AHMP-AuNPs coming closer and leading to aggregation. Overall, the higher pH value induces the aggregation of AHMP-AuNPs. By the influence of OH^- ions, the UV-Visible spectrum of the AHMP-AuNPs shifts to the higher wavelength side (red shift). In pH 8, the AHMP-AuNPs shows a sharp peak at 522 nm with medium intensity because the OH^- ion counts are decreased at pH 8 rather than pH 9 and hence the newly formed negative-negative repulsion is reduced and hence the blue shift is observed (28 nm) compared to pH 9. The overall results indicate that pH 7 is the best choice for preparing AHMP-AuNPs in terms of its stabilization.

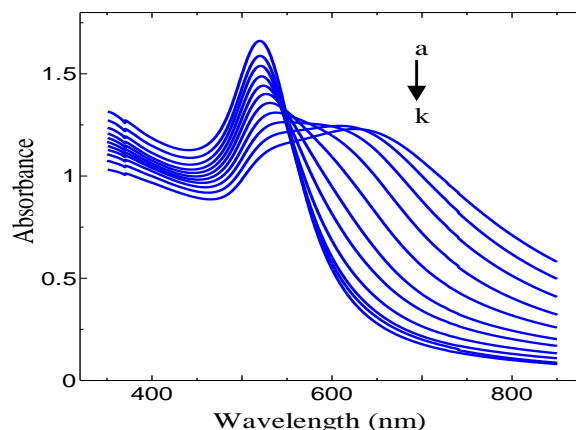


Fig. 2. Effect of salt addition: Absorption spectra obtained for (a) 0.00 M (b) 0.01 M (c) 0.02 M (d) 0.03 M (e) 0.04 M (f) 0.05 M (g) 0.06 M (h) 0.07 M (i) 0.08 M (j) 0.09 M and (k) 0.10 M NaCl solution.

3.2. Effect of salt on AHMP-AuNPs

Further, the stability of the AHMP-AuNPs is investigated by the addition of salt (NaCl). Fig. 2 shows that the UV-Visible spectra for the effect of salt addition in AHMP-AuNPs. The effect of NaCl addition is checked from the preparation of 0.01 M to 0.1 M with an interval of 0.01M for AHMP-AuNPs. When the addition of 0.01 M NaCl, the intensity of the SPR band is reduced and slowly moves towards higher wavelength side (red shift) in UV-Visible spectrum. Generally, the addition of salt induces the increase the size of the nanoparticles which implies the slow aggregation. The similar trend is observed in the present study. The remaining solution of 0.02 M to 0.1 M also tested in the similar way. While the increase the amount of NaCl in the AHMP-AuNPs clearly indicating the red shift due to aggregation. In certain points (0.09 M & 0.1 M NaCl), UV-Visible spectrum shows two peaks for AHMP-AuNPs which indicating while aggregation forms a new anisotropic structures are formed. First hump is around 530 nm and second hump around 610 nm indicating the aggregation of AHMP-AuNPs in addition with formation of anisotropic structures. Hence, the addition of salt gradually induces the slow aggregation of AHMP-AuNPs.

3.3. Morphological studies of AHMP-AuNPs by HR-TEM and XRD and AHMP-AuNPs modified ITO by AFM

The morphology and the size of the synthesized AHMP-AuNPs were done by HR-TEM analysis. Fig. 3 shows that the HR-TEM images of AHMP-AuNPs in the cross section of 50 nm (3a) and 10 nm (3b), 5 nm (3c) and 2 nm (3d), respectively. A spherical like shapes particles were observed in the HR-TEM images for AHMP-AuNPs. When measuring the size of the AHMP-AuNPs, the average size of 6-8 nm was observed which is proved that the AHMP-AuNPs are in the nanosize. AHMP-AuNPs has appeared in the crystalline nature, whereas, some of the particles were found in agglomeration condition.

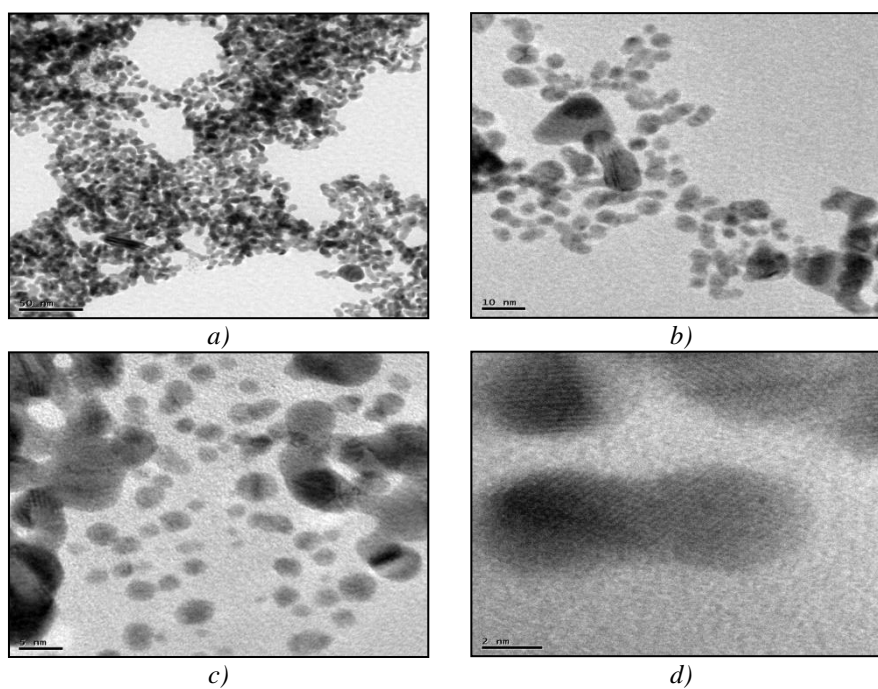


Fig. 3. HR-TEM images of AHMP-AuNPs in the cross-section of
a) 50 nm, b) 10 nm, c) 5 nm, d) 2 nm

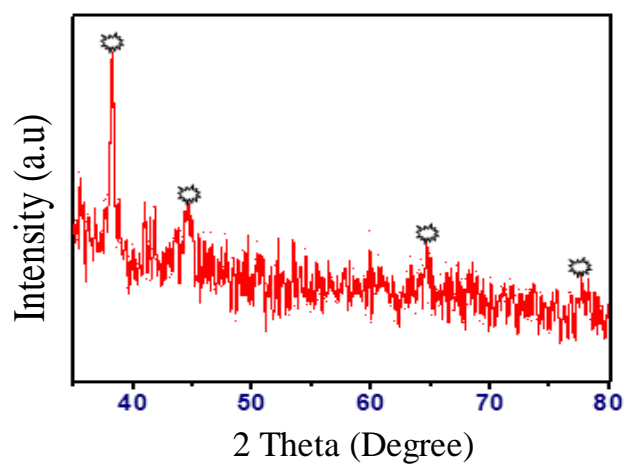


Fig. 4. XRD pattern of AHMP-AuNPs.

Fig. 4 shows XRD pattern of AHMP-AuNPs and it gives high intensity peaks. The Bragg reflections in the 2θ are 38.1, 44.2, 64.6 and 77.4 which are representing the lattice space of 111, 200, 220 and 311. The Bragg reflections indicating the AHMP-AuNPs is exist as face center cubic lattice (FCC).

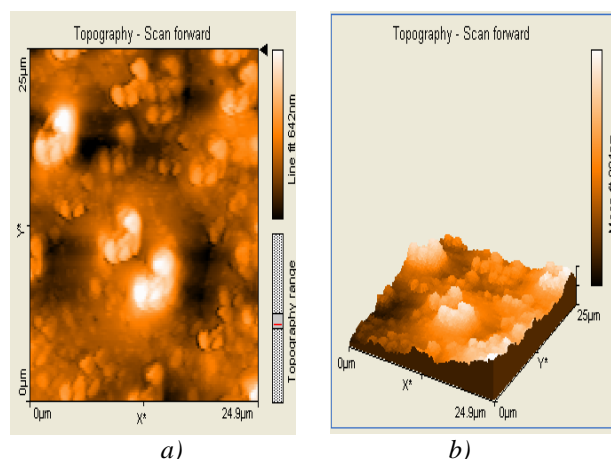


Fig. 5. AFM images of modified AHMP-AuNPs substrate. (a) Topographical view (b) 3-Dimensional view

Further, the modification of AHMP-AuNPs/MPTS/ITO substrate was confirmed by its surface morphology using AFM. Fig. 5 shows AFM images of AHMP-AuNPs modified substrate in topographical (a) and 3-D view (b). It shows well-dispersed, homogeneously shaped particles with spherical nature. The thickness of the layer is 400 nm and it shows the uniform coating on the ITO surface.

3.4. Electrocatalytic applications towards NEP and UA determination

Physiological pH is very important for clinical analysis because EP and UA present in human fluids such as blood serum and plasma. Therefore, pH 7.2 was selected for the determination of EP and UA. Moreover, AHMP-AuNPs are also prepared at pH 7 for application point of view. Fig. 6 shows the cyclic voltammograms (CVs) obtained for 0.5 mM EP (blue), UA (red) and absence of both EP and UA (brown) at AHMP-AuNPs/MPTS/ITO electrode in 0.2 M PB at a scan rate of 50 mV s^{-1} . The modified electrode shows an oxidation peak at 0.21 V and a reduction peak at 0.13 V with a ΔE_p of 80 mV was observed (blue). The observed less ΔE_p indicates that the electron transfer reaction of EP was faster at AHMP-AuNPs/MPTS/ITO electrode. The UA oxidation peak for AHMP-AuNPs/MPTS/ITO electrode at 0.51 V (red) was observed. Hence, the observed CV of EP and UA indicate that the electrochemical determination of EP and UA is possible at AHMP-AuNPs/MPTS/ITO electrode.

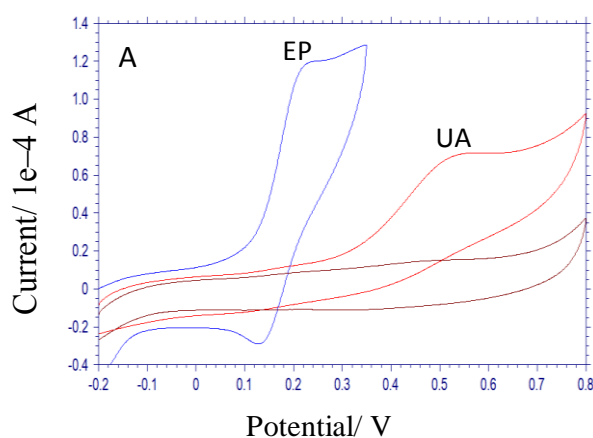


Fig. 6. CV for 0.5 mM EP and UA at AHMP-AuNPs/MPTS/ITO electrode for EP (blue), UA (red) and absence of EP and UA (brown).

Since two of these analytes are available in human fluids and their concentrations are responsible for many diseases, the simultaneous determination of EP and UA is essential. Hence, we have attempted to determine simultaneously using present modified electrode. Fig. 7 shows the differential pulse voltammograms (DPVs) for each addition of 5 μM EP and 20 μM UA at AHMP-AuNPs/MPTS/ITO electrode (curves a-c) in 0.2 M PBS (pH 7.2). The oxidation peak obtained for EP at 0.15 V and UA at 0.34 V at modified electrode (curve a) in first addition, clearly indicates the low concentration of simultaneous determination is possible at AHMP-AuNPs/MPTS/ITO electrode. The voltammetric signals of EP and UA with a potential difference of 190 mV along with enhanced oxidation peak currents. Further additions (curves b-c) of EP and UA shows the uniform increases of current without change any potential indicates the good stability of the electrode. Thus, AHMP-AuNPs/MPTS/ITO electrode was more suitable for the simultaneous determination of EP and UA.

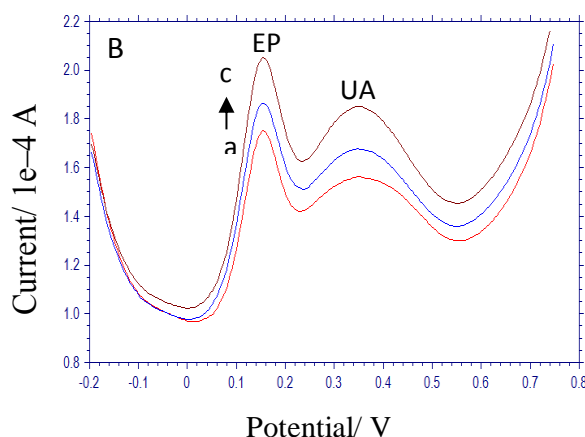


Fig. 7. DPVs for the each increment of 5 μM EP and 20 μM UA (curves a-c) at AHMP-AuNPs/MPTS/ITO electrode.

4. Conclusion

In this work, the pH investigation of AHMP-AuNPs in different pH conditions such as pH 3–pH 9 to find the optimization point for the benefit of electrocatalytic application. The result shows that pH 7 is the ideal condition of AHMP-AuNPs stabilization rather than other pH. This is because the presence of lone pair of electrons in the amine groups of the monomer (AHMP) generates the electrostatic repulsion between the adjacent AuNPs surfaces which stabilized from aggregation of AHMP-AuNPs at neutral pH. The salt effect experiment indicates that the addition of salt induces the slow aggregation of AHMP-AuNPs. Moreover, no influence of H^+ and OH^- ions at pH 7 and hence AHMP-AuNPs are well stabilized by their capping agent in this range. The spherical shape with average size of 6–8 nm size of AHMP-AuNPs was confirmed by HR-TEM images. Using XRD result, the Bragg reflections of 2θ are 38.1, 44.2, 64.6 and 77.4 indicating the AHMP-AuNPs exist in the lattice space of 111, 200, 220 and 311. Further, AHMP-AuNPs are fabricated on ITO substrate using MPTS linker and the surface. The resultant AHMP-AuNPs/MPTS/ITO electrode was probed by AFM method and it shows 400 nm thickness of layer. Finally, the modified electrode is used for the electrocatalytic application of epinephrine (EP) and uric acid (UA). In CV method, the oxidation peak at 0.21 V and a reduction peak at 0.13 V with a ΔE_p of 80 mV were observed for EP and 0.51 V oxidation peak observed for UA at AuNPs/MPTS/ITO electrode. Finally, the simultaneous determination of EP and UA is also successfully achieved by using the modified electrode. The oxidation peak obtained for EP at 0.15 V and UA at 0.34 V at modified electrode by DPV method.

Acknowledgements

Dr. S. Brillians Revin, thanks to Anna University Recognized chemistry research centre, Department of chemistry, Francis Xavier Engineering College for their constant support. I extend my sincere thanks to Dr. S. Abraham John, Professor, Department of Chemistry, Gandhigram Rural Institute, India, for his encouragement.

References

- [1] N. Li, P. Zhao, D. Astruc, *Angewandte Reviews* **53**, 1756 (2014).
- [2] C. Kohout, C. Santi, L. Polito, *International Journal of Molecular Sciences* **19**, 3385 (2018).
- [3] M. Sengani, A. M. Grumezescu, V. D. Rajeswari, **2**, 37 (2017).
- [4] M. Sharon, A. Mewada, N. Swasminathan, C. Sharon, *Nanomeicine and nanotechnology Journal* **1**(1), 113 (2017).
- [5] P. Priece, H. A. Salami, R. H. Padilla, Z. Zhong, J. A. Lopez-Sanchez, **37**, 1619 (2016).
- [6] M. H. Jazayeri, T. Aghaie, A. Avan, A. Vatankhah, M. R. S. Ghaffari, *Sensing and Bio-sensing Research* **20**, 1 (2018).
- [7] L. Kool, A. Bunschoten, A. H. Velders, V. Saggiomo, *Beilstein Journal of Nanotechnology* **10**, 442 (2019).
- [8] M. A. Raj, S. B. Revin, S. A. John, *Colloids and surfaces B Biointerfaces* **87**(2), 353 (2011).
- [9] S. Shankar, S. A. John, *RSC advances* **5**, 49920 (2015).
- [10] J. M. Sullivan, R. Gorlin, *Circulation Research* **21**(6), 9191 (1967).
- [11] L. I. Goldberg, R. D. Bloodwell, E. Braunwald, A. G. Morrow, **22**(6), 1125 (1960).
- [12] N. Ballin, Bernard Becker, M. L. Goldman, *Investigative Ophthalmology* **5**(2), 165 (1966).
- [13] F. K. Heath, *The American Journal of Medicine* **9**(6), 799 (1950).
- [14] G. Ragab, M. Elshahaly, T. Bardin, *Journal of Advanced Research* **8**(5), 495 (2017).
- [15] G. Karim-Nezhad, Z. Khorablou, *Analytical Methods* **45**(9), 6394 (2017).